ISSN 2563-9218

RESEARCH ARTICLE

Analysis of Red Blood Cell Samples using a Handheld Shear-horizontal Surface Acoustic Wave Biosensor

Marlon S. Thomas*

Thomas MS. Analysis of Red Blood Cell Samples using a Handheld Shear-horizontal Surface Acoustic Wave Biosensor. Int J Biomed Clin Anal. 2023;3(1):01-12.

Abstract

Human red blood cells (RBCs) are highly studied by researchers and clinicians alike because RBCs play an essential role in medical diagnostics. RBCs are the most abundant component of whole blood. The accurate analysis of blood samples for blood cells is crucial to help diagnose and management of several life-threatening diseases. Current techniques for analyzing blood cell counts are time-consuming and expensive, requiring a highly trained technician. Implementing a portable, label-free method enables analysis at small clinics and remote locations with reduced times of analysis and cost. The development of miniature, handheld shear-horizontal surface acoustic wave (SH-SAW) biosensors capable of accurately counting RBCs in liquid samples will improve medical diagnostics in resource-limited regions of the United States and parts of the world where access to centralized clinical laboratories is limited. A shear-horizontal surface acoustic wave is a horizontally polarized surface acoustic wave that is produced by a transducer that is fabricated onto a piezoelectric substrate such as lithium tantalate, lithium niobite, or quartz. We report a lithium tantalate SH-SAW biosensor and method for monitoring the RBC level (hematocrit level) from a whole blood sample using a shear-horizontal surface acoustic wave (SH-SAW) biosensor that uses a 500-picoliter sample well. Samples were introduced by directly pipetting whole blood onto the sample reservoir and washing away any excess material. The SH-SAW biosensor uses an immunoassay, where the antibody anti-glycophorin A is coated on the surface of the active area of the sensor. The sample is compared to a reference sample. Using Microsoft Excel statistical tools, we showed that the results demonstrate the concentration dependence of the samples with an average coefficient of variance (CV) within a sample group was 10% or less for all samples analyzed. Our successful demonstration offers proof of concept for handheld blood cell monitors for remote and resource-limited applications. To our knowledge, this is the first demonstration of an SH-SAW device being used for monitoring red blood cell counts.

Key Words: *Shear-horizontal surface acoustic wave; Biosensor; SH-SAW; Microfluidic; Red Blood Cells (RBCs)*

Assistant Professor of Bioengineering Program, Fisk University, Nashville, Tennessee 37208, United States

**Corresponding author: Marlon S. Thomas, Assistant Professor of Bioengineering Program, Fisk University, Nashville, Tennessee 37208, United States, Tel: 5627258930; E-mail: msthomas@fisk.edu*

Received: December 18, 2022, Accepted: January 30, 2023, Published: March 03, 2023

Introduction

Human blood, like all other animals, contains many constituents. Human blood components include several blood cells, including the three most common types of blood cells, red blood cells (erythrocytes), white blood cells (leucocytes), and platelets (thrombocytes) [1,2]. However, red blood cells (RBCs) are the most abundant blood cell type and their concentration in the blood is critical to ensure the proper transporting of oxygen to all areas of the body. RBC counts allow doctors to predict a patient's condition and monitor a patient's progression. The accurate analysis of blood samples for blood cells is a crucial step to help diagnose diseases like malaria or for monitoring blood disorders like anemia, which is related to the production and destruction of the Porphyrin group in red blood cells, which facilitates the oxygen-carrying capacity of hemoglobin in RBCs [3-5]. As a result, counting blood cells is among the most used routine tests in diagnostic medicine. The manual method of counting blood cells, using a hemocytometer, is both cumbersome and time-consuming while having poor accuracy and precision [6]. A reduced number of red blood cells in circulation can result in anemia, which can be caused by genetic conditions such as sickle cell anemia [7,8] or chemotherapy [9,10]. The consequence of anemic conditions is the reduction in Hematocrit [11]. RBCs have some glycoproteins in their cell membrane, such as glycophorins A - D, that are present in all mature RBCs [12]. Glycophorin A (glycophorin alpha) occurs naturally as a dimeric complex and is a significant component of RBC cell membrane glycoproteins with a molecular weight of 31 kDa [13-15].

The methods for counting blood cells vary but most involve separating blood cells into individual components via centripetal force and then analyzing the fractions by one of three primary methods. The original method of counting RBCs, as previously mentioned, was to use a hemocytometer, which involved using a small glass object with a very precise volume, and counting using a hand counter hemocytometer [6]. Since all steps are manual, counting cells in this manner is laborious. In 1956, the first blood-automated cell counter was introduced by the Coulter brothers, Wallace H. Coulter and Joseph R. Coulter [16-18]. The Coulter brothers introduced the Coulter principle, which became the standard method that the majority of blood cell counters have been based on since that time. They later founded Coulter Electronics, Incorporated in 1958 [16-18]. The original design was to feature blood cells being counted as they flow down a capillary tube, passing through a light beam, however, due to technical difficulties, they settled for using an orifice in a J tube [16,17]. Developments and refinements of the ideas developed by the Coulter Cooperation led to the development of four methods for counting blood cells. These included using a Coulter counter, flow cytometry, and hematology analyzer which incorporated concepts from both the Coulter principle and flow cytometry and imaging-based techniques using the original hemocytometer with more sophisticated grids and incorporated a microscope [19,20]. When counting RBCs using a Coulter counter, individual RBC cells are passed through an orifice where an electric current is flowing from an electrode out of the tube to an electrode inside the tube [5,21]. The detection of the cell is based on the difference in electrical conductivity as the cell passes through the orifice [18]. As the RBC passes, it changes the resistance in the circuit, resulting in a voltage drop across the current path and referred to as a resistive pulse [22]. The amplitude of the resistive pulse is associated with the size of the RBC [22] while the histogram showing the

total number of pulses is the overall number of RBCs in a given separated blood sample [22]. Developments from the refinement of automated Coulter counters led to the development of the original idea by Wallace Coulter which became known as the Flow-activated cell counters or flow-activated sorting counts cells [23]. One of the primary developments was the introduction of a flowing stream focused on a sheath flow [6-10]. The analysis of RBCs by imaging represents the most popular method of RBC analysis [11]. This method typically uses a sample with a precise volume that is delivered over a grid. Cells in the grid are counted following a protocol [24-28]. Many problems are related to studying microscopy images, such as RBCs. This includes images from hemocytometers, blood smears, and other image-based techniques. While highly utilized in both clinical and research laboratories, the methods listed above are time-consuming and costly due to the requirement for specialized, dedicated equipment and a well-trained technician. For these reasons, alternative strategies are examined as rapid, portable, and cost-effective for resource-limited environments [29]. Recently, Shengbo Sang and colleagues at the Taiyuan University of Technology reported a portable microsystem that integrates multifunctional dielectrophoresis was used to separate lysed RBCs from viable RBCs [30]. The method employs several methods to achieve cell separation. The capacitance of the dead cells and live cells were different so a ratio could be established. However, the method was not designed to obtain absolute RBC counts but rather to distinguish the ratio of lysed to non-lysed RBC in the blood of patients suffering from hemolytic anemia [30].

In this study, we explored the detection of RBCs using a Shear Horizontal (SH) Surface Acoustic Wave (SAW) Biosensor system. The SH-SAW biosensor is a label-free direct measurement that offers real-time reporting of immunoassays [12]. The immunoassay works by targeting the glycophorin A glycoproteins on the RBC surface [31,32]. Antibodies immobilized RBCs against glycophorin A. Here we demonstrated the ability of the SAW system to detect RBCs in a concentrated solution and dilutions over three orders of magnitude. The time to detection was less than 5 minutes. This represents a critical step toward the realization of portable point care diagnostic (POC) diagnostic tools for detecting RBCs and other blood cells.

Materials and Methods

Reagents

The reagents used in this study are listed below and were used without any further purification: (3-Glycidoxypropyl) Trimethoxysilane (GPTMS), >99%, anhydrous from Gelest Inc., Cat#SIG5840.1; Toluene, 99.85%, Extra Dry over Molecular Sieve from AcroSeal™, ACROS Organics™ via Fisher Scientific, Cat#AC364415000; StabilCoat Immunoassay stabilizer, from Surmodics, Cat#SC01-0050; 10x Phosphate buffered Saline Cat#AAJ62036K7 was purchased from ThermoFisher and diluted with sterile deionized water to 1x and filtered with a 0.2 micron filter before use, ThermoFisher filter bottle Cat#09-741-03, Sodium bicarbonate from Amresco, Cat#0865-1kg; Sodium carbonate, anhydrous from Sigma Aldrich, Cat#223484-500G; Sodium phosphate monobasic anhydrous from Amresco, Cat#0571-500g; Potassium phosphate monobasic from Fisher Scientific, Cat#P285-500; Sodium chloride from Sigma Aldrich, Cat#S6191-500g; Ethylenediaminetetraacetic acid (EDTA) from Sigma Aldrich, Cat#E6758-100G; Glycerol from Alfa Aesar, Cat#32450; and Sterile Deionized water (18 MΩ Deionized water). Antibodies against glycophorin A were obtained from BD Biosciences Cat#340947. Mouse F(ab')2

IgG1-Isotype Control; Abcam, Cat#ab37426, Packed RBC sample was obtained from BioIVT Cat#NormalHumanRBCK2UZN. SH-SAW R1 reader (Sandia National Laboratory), Oven (ThermoFisher), Compressed nitrogen 99.9% pure (Airgas), Desiccator, Chemical Hood, Vortex mixer (Fisher Scientific), Disposable gloves, and eye protection.

The SH-SAW System

The SH-SAW device generates a surface acoustic wave in a piezo-electric, lithium tantalate substrate. The acoustic wave is generated by exciting a pair of interdigitated transducers (IDT) via an applied radio frequency of 325MHz [33]. The electromechanical coupling between the lithium tantalate substrate and the input IDT sends a traveling surface wave through the substrate [34-36]. The IDT design allows unidirectional propagation of the acoustic wave from one pair of IDT across a "delay line" on the substrate and is received by another IDT positioned at the opposite end of the delay line [37-39]. The wave has two components, one normal to the SAW propagation (the longitudinal component) and one parallel (the shear component). A thin film of silicon dioxide (SiO_2) deposited over the "delay line" serves as a guiding layer to confine the SAW to the surface of the chip [33,40]. The guiding silicone dioxide layer coated on the substrate minimizes vibration energy losses into the liquid on the surface and confines the "detection zone" to a thin layer above the sensor's surface [41]. Computational modeling of a homogeneous biological layer captured on the sensor's character suggests that the "detection zone" is approximately 30nm from the sensor surface into the plain [42-44]. Changes in properties of the sensor surface and adjacent solution within this detection zone alter the travel time and amplitude of the wave. The perturbation of the wave velocity results in a shift in the frequency between the two IDTs as the acoustic wave propagates across the delay line. The measured phase shifts across the delay line are reported. Small changes in the surface viscosity and alterations in the density of the bulk solution are readily detected by observing the phase delay and amplitude of the acoustic wave relative to the reference signal [45,46]. By functionalizing the substrate with an antibody specific to a target analyte, we can register changes in the concentration of the immobilized target as a change in the phase and amplitude of the detected RF signal; this is the basis of measurement with the SAW system [45,47,48].

We used a shear-horizontal surface acoustic wave (SH-SAW) sensor and reader, developed at Sandia National Laboratory to perform counting of RBCs at different levels of dilution. The SAW device uses a SAW chip designated as model S1. The S1 sensors have four identical channels with delay lines with a pair of IDTs at either side of the delay line, as seen in Figure 1. The topmost surface of the SAW chips is coated with a 500 nm layer of SiO_2 to: confine the acoustic wave to the $LiTaO_3$ surface, prevent leakage of the acoustic wave into the liquid, and protect the metalized areas from harsh chemicals [49]. The standard configuration of the test is to use three lanes as active sample lanes and to designate one lane as a reference lane to account for environmental changes. The first three lanes are coated with the same anti-glycophorin A monoclonal antibody (mAb) in preparing the sensor for an experiment, and the fourth channel is coated with a reference material, a non-binding antibody that does not target the glycophorin A antigen (a mouse F(ab')2 IgG1 from Abcam Biotechnology company). The reference lane is further conditioned by saturating it with the target analyte of interest and cross-linking to prevent dissociation. The SNL R1 reader has an RF source (Valon 5009), and data is acquired

using a NI DAQ (National Instruments 9205) module interfaced via USB to a desktop PC. The RF source, reader board functionality, and data acquisition functions are controlled via a customized graphical user interface (GUI) developed for the SH-SAW reader. For testing, the SH-SAW sensor is placed in a temperature-controlled chamber. The biosensor was able to accurately monitor a RBC sample and dilutions down to 99.9% of the starting RBC sample.

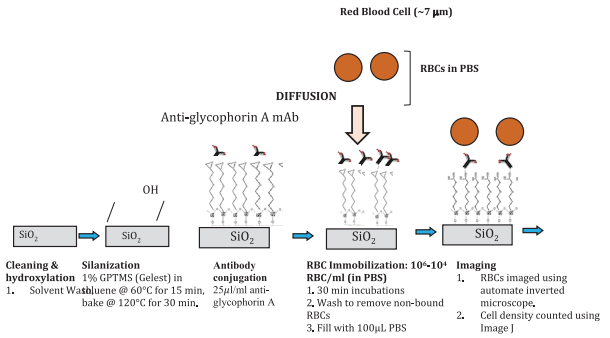

Figure 1) *Schematic of the overall immunoassay for the capture of red blood cells. The viscoelastic changes induce a phase shift on the SH-SAW biosensor. A mild wash is used to ensure surface induces that excess loose cells are not captured.*

QC and salinization of SH-SAW chip

Prior to chemical preparation, all sensors were subjected to the following QC protocol. First, sensors were inspected for dust, chemical residues, and/or scratches using a stereomicroscope, and images were recorded. Next, a frequency sweep was performed in the air reader GUI to examine the proper electromechanical functionality of the SH-SAW sensor. In a normal sensor chip, the signal received from all four channels during this scan was displayed as equivalent overlapping saw-tooth waveforms. The sensor passes QC when all channels exhibit an output waveform with a similar time course and amplitude.

To prepare the chips for an experiment the first step involves salinization of the SH-SAW S1 sensor (Figure 2) via vapor deposition and a select number of sensors were also coated using solution chemistry. The SAW chips were first pre-cleaned in a UV-Ozone cleaner for 15 minutes to remove organic residues. A fresh mixture of 1%v/v GPTMS in toluene was then prepared in a clean glass vial and left at room temperature for 5 minutes to allow hydrolysis of the silane. The chip was then removed from the Ozone treatment and submerged in the 1%GPTMS-toluene solution and incubated for 15 min at 60°C in a pre-heated vacuum oven. Silanized chips were then rinsed (right-side-up) with toluene 3x times, dried with N_2, transferred to a clean glass vial, and baked at 120°C for 30 min in a vacuum oven. Samples were then removed and allowed to cool to room temperature for 15 min before use. All salinized S1 sensors were stored in a desiccator and used within 2 weeks of preparation.

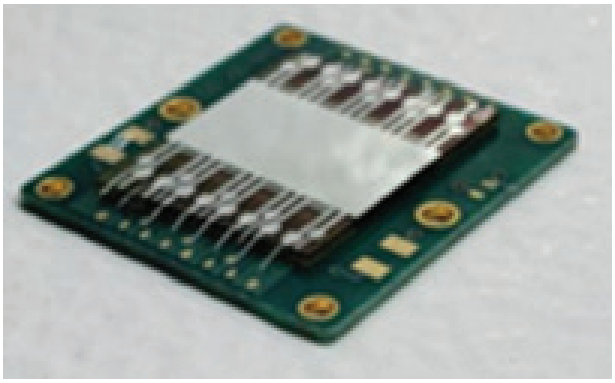

Figure 2) *Photographs of the S1 sensor for the R1 SH-SAW reader.*

Preparation of packed RBC serial dilutions

The RBCs were purchased from BioIVT supplied at a stock concentration of $6x10^6$ Cells/mL (as stated by BioIVT) in an aqueous solution of Phosphate buffered saline pH 7.4 supplemented with 5 mM EDTA as an anticoagulant. The diluted samples were prepared fresh before each experiment.

Functionalization to enable capture of RBC in the SH-SAW sensor surface

In this experiment, the goal was to detect RBC cell particles by binding to a detection

mAb immobilized on the SAW chip. The functionalization of the sensors was carried out using a customized conjugation fixture, which allowed each lane to be functionalized individually. This is critical because at least one lane must serve as a reference lane and therefore must be functionalized using a different protocol and using a non-binding antibody fragment (discussed below). In these experiments, two channels (lanes 3 and 4) were used as references.

To functionalize the sensors, stored silanized chips were first placed in the customized conjugation fixture. The silanized SH-SAW chip was oriented so that the Sandia Thunderbird logo was positioned at the top, thereby placing lanes 1 through 4 from top to bottom. Subsequently, 25µL of anti-HA mAb diluted to 100µg/mL in 100mM $NaHCO_3/Na_2CO_3$ buffer at pH 9.2 was added to lanes 1-3 and incubated at room temperature for 60 minutes. Likewise, the F(ab')2 IgG for the reference lane was diluted in 100 mM $NaHCO_3/Na_2CO_3$ buffer at pH 9.2, added to lane 4, and incubated under the same conditions. After incubation and with the sensors in the fixture, the wells were washed twice with 100 mM Na_2HPO_4/NaH_2PO_4 buffer at pH 7.4 with 0.05 v/v% TWEEN®-20 and then twice with buffer without TWEEN®-20. Immediately after, 25µL of StabilCoat® was added to all channels, incubated at room temperature for 10 minutes, and washed by DI water (Figure 3). StabilCoat® accomplishes the following: it saturates unbound epoxide groups on the surface that was not already bound to the mAb to reduce nonspecific binding, it stabilizes proteins by maintaining the proper osmotic pressure of the protein bound to the surface, and it promotes mAb stability and function for drying and storage. Functionalized SH-SAW sensor chips are referred to as biosensors from this point forward. At this point, the biosensors were ready for testing.

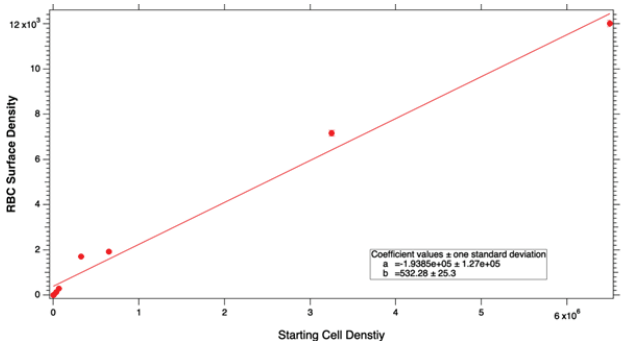

Figure 3) *The plot of the experimental data from the experiments. The x-axis gives the RBC surface density while the y-axis gives the starting RBC number counts. Error bars represent the standard deviations. All data points were done in quadruplets and the error bars represent the standard deviation from the mean value. The R^2 for the linear fit was $R^2 = 0.99$.*

SH-SAW System setup and calibration

Prior to each experiment, all biosensors are evaluated for response and sensitivity. A test sweep is performed by scanning between a range of frequencies from 324-326 MHz. The acoustic wave is generated by exciting a pair of interdigitated transducers (IDT) via an applied radio frequency of 325 MHz. The electromechanical coupling between the lithium tantalate substrate and the input IDT sends a traveling surface wave through the substrate. The IDT design allows unidirectional propagation of the acoustic wave from one pair of IDT across a "delay line" on the substrate and is received by another IDT positioned at the opposite end of the delay line. The SAW has two components, one normal to the SAW propagation (the longitudinal component) and one parallel (the shear component), however, the piezoelectric substrate that generates the SAW is cut to allow only the shear component. Therefore, the sensors become horizontally polarized and the longitudinal component of the wave is suppressed. The longitudinal component of the wave is severely dampened by liquids. A thin film of silicon dioxide (SiO_2) deposited over the delay line serves several

critical functions. First, it serves as a guiding layer to confine the SAW to the surface of the chip. The guiding silicone dioxide layer coated on the substrate minimizes vibration energy losses into the liquid on the surface and confines the "detection zone" to a thin layer above the sensor's surface. Computational modeling of a homogeneous biological layer captured on the sensor's character suggests that the "detection zone" as mentioned before, is approximately 30 nm. Changes in properties of the sensor surface and adjacent solution within this detection zone alter the travel time and amplitude of the wave. The perturbation of the wave velocity results in a shift in the frequency between the two IDTs as the acoustic wave propagates across the delay line. The measured phase shifts across the delay line are reported. Small changes in the surface viscosity and alterations in the density of the bulk solution are readily detected by observing the phase delay and amplitude of the acoustic wave relative to the reference signal. By functionalizing the substrate with an antibody specific to a target analyte, we can register changes in the concentration of the immobilized target as a change in the phase and amplitude of the detected RF signal; this is the basis of measurement with the SAW system.

Prior to each SH-SAW measurement, the SH-SAW reader was placed in an environmental chamber pre-heated to 35°C for 60 mins, on a vibration isolation platform, and with the RF source powered for at least 15 minutes to minimize environmental effects. To set up the experiment, a biosensor was selected at random and loaded into the adapter on the SAW system. Then, 107µL of 6.4mM $NaHPO_4$, 3.3mM KH_2PO_4, 100mM NaCl, and 5mM EDTA at pH 7.0 was added uniformly to the sample well by pipetting action and the system was visually inspected for leaks. A frequency sweep was carried out once again (this time in a wet environment) to confirm adequate biosensor response and to establish an operating frequency (i.e., calibration) for phase measurement. The addition of liquid causes the amplitude of the waveform to drop considerably due to the change in permittivity of the water and its effect on the localized electric field of the SAW wave. Thus, in a wet frequency sweep, the saw-tooth peaks and valleys become rounded and asymmetric due to loading by the liquid. A properly operating biosensor showed similar phase slopes for all four channels with minimal attenuation and the operating frequency was selected based on the point of maximum congruency for all four channels on a given sensor. In the case of incongruent channels, the biosensor was discarded and replaced with another biosensor. The phase slope (i.e., phase/frequency) value has been indicated to provide a measure of the sensitivity of SH-SAW biosensors.

SH-SAW phase measurement

After establishing the operating frequency (i.e., calibration), the buffer temperature was stabilized for 10 minutes to obtain a stable phase response baseline of approximately 0.2°. Data acquisition was then initiated, and 5µL of the diluted RBC sample solution was added to the buffer in the well after 30 seconds of baseline measurement. Data acquisition was collected for 10 minutes for each run. After each measurement, the sample well was washed twice with 100 mM PBS at pH 7.4 with 0.05 v/v% TWEEN®-20 and then twice with PBS without TWEEN®-20. Control experiments to validate the specificity of RBCs were performed and compared with the response against wild-type anti-glycophorin A. Likewise, we evaluated the effect of glycerol for sample delivery to verify the phase separation approach.

Data analysis

Each phase measurement was run in quadruplets. The SH-SAW biosensor system produces phase shift values for each channel individually recorded as a function of time. All data analysis performed in this study used end-point analysis, where the phase values at discrete time points were used to quantify the response to the addition of the RBC sample solution. The ending point values from each channel were obtained by averaging phase values for 5 seconds after a 10-minute incubation.Subsequently, the average from the reference channel was subtracted from each active channel to yield a phase shift relative to the reference.

Results

The results show that the SH-SAW biosensor can detect a monolayer of RBCs on the sensor's surface in a concentration-dependent manner. The sensor can measure as little as 13 cells to as many as 12,014 cells. The sensor's surface area becomes saturated and limits our ability to add additional cells. The selective manner in which the cells are immobilized to the sensor (Figure 4) means that the sensor is capable of probing for any blood cell type and is capable of multiplexed measurement, i.e., up to three different blood cells can be measured simultaneously. Designs are being developed to simultaneously enable the multiplexing of up to five cell types.

It is critical to develop an automated sequential process so that all the sensors are processed in an identical manner each time. If not, human error could induce slight variations in the measurements. However, the data show a strong linear correlation between the S1 surface density, and the phase shifts recorded by the R1 reader.

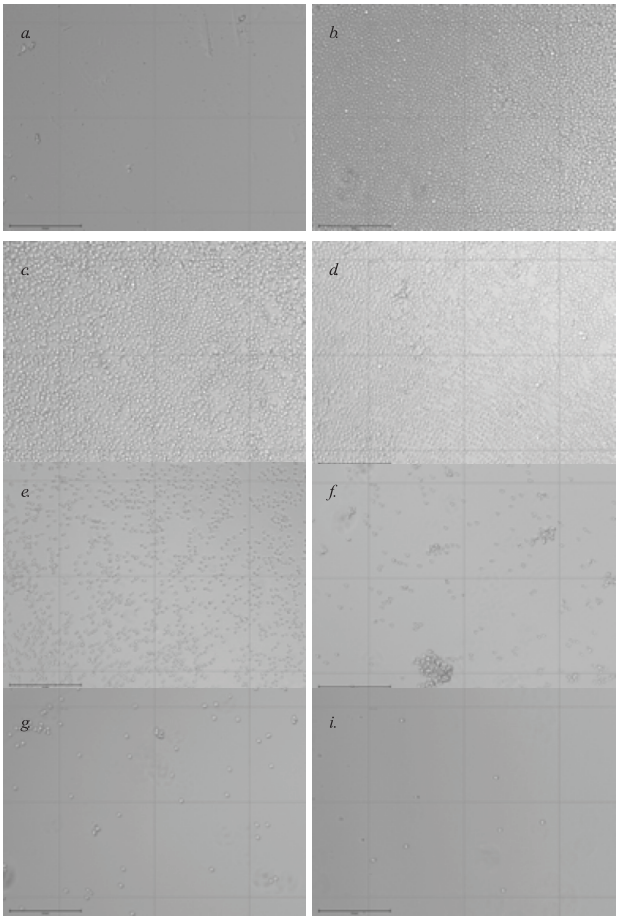

Figure 4) *Representative images of RBCs immobilized on the surface of the biosensor with an anti-glycophorin and an anti-glycophorin A antibody. The anti-glycophorin A antibodies were coated at a concentration of 25g/ml and incubated for 15 minutes on the organosilane (3-Glycidyloxypropyl) trimethoxysilane (GPTMS). The figure shows a surface density resulting from having a starting concentration with packed whole blood (a) 6.5x10^6 RBC/μl (b) 3.25x10^6 RBC/μl (d) 5%RBC (e) 1% (f) 0.5%RBC (g) 0.1%RBC solution and (i) is phosphate buffered saline (PBS) solution. The antibody-coated surface is rinsed with PBS before and after usage.*

The comparison was made to establish the correlation between the phase shift and the RBC counts. The observation that the measured phase shift is directly proportional to the number counts of cells on the surface of the sensor after washing, implies that an SH-SAW biosensor reports a phase shift that directly measures the number of RBCs bonded to the surface of the sensor. This result was unexpected given the highly non-linear nature of SAW devices. However, the size and mass of the RBCs are

such that they do not have a large mass and so the sensor only sees a minor perturbation due to RBCs bound, after the removal of the excess cells. Since the number of RBCs bound is directly proportional to the phase shifts, a correlation between the RBC cell number to induced phased shifts was established. The ratio of the slopes establishes this correlation, and it gives a result that estimates that the SH-SAW measures 1 degree in phase shift for every 237 RBC cells bound to the surface. Therefore, the SH-SAW device increases by one degree with every 147 RBC added in a linear fashion from approximately 13-12,000 and shows no sign of saturating. The linear dynamic range for measuring bound RBCs is therefore quite large, relative to other techniques for performing cell counts. Since the SH-SAW is calibrated to measure down to 10 milli-degree (m-degree), we can theoretically measure 2 red blood cells. A more accurate measurement could be made of ~5 RBCs, which would generate will ~20m-degree in phase shift. This is seen graphically in Figure 5.

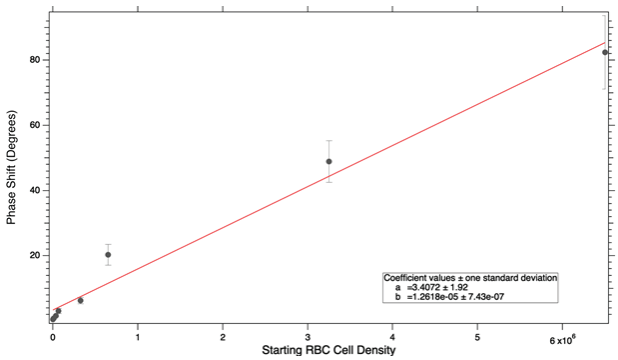

Figure 5) *The plot of the phase shift as a function of the starting the starting RBC cell counts. All data points were performed in quadruplets and the error bars represent the standard deviation from the mean value. The R^2 for the linear fit was R^2=0.98.*

Conclusion

The first successful demonstration of a handheld SH-SAW biosensor that is able to accurately and quantitatively determine RBC concentration in real-time. The device demonstrated the capability to the determination of RBC cell densities in the presence of a PBS solution over a concentration range spanning three decades. Such an instrument could provide vital information for patients who are anemic due to an infection or due to the patient having a genetic trait. The handheld SH-SAW biosensor would be perfectly suited to evaluate changes in RBC levels due to medical treatment or even an acute allergic reaction. We believe that our SH-SAW biosensors will be able to improve patient care in a spectrum of settings for either acquired or congenital conditions. Our device may enable the simultaneous monitoring of multiple blood cell types from a 0.5µL blood sample. This could be achieved from a small finger prick or a micro-needle sample including small clinics, resource-limited hospitals, and at-home applications. Our device can potentially change how medicine is practiced in resource-rich and resource-limited areas by enabling the personalization of medical diagnostics. It could start to offer a democratization of personalized medicine where anyone can determine their blood cell counts, such as HIV^+ patients and some cancer patients. They would complement point-of-care testing protocols that have enabled the rapid assessment of patients to increase the speed at which intervention is achieved. Analyzing peripheral blood samples from a finger prick can become a standard in medical diagnostics. Funding for this work was provided by the United States National Science Foundation (NSF), grant number 1817282, and the United States Department of Energy (DOE), grant number 620035.

References

1. Sudakevitz D, Levene C, Sela R, et al. Differentiation between human red cells of Pk and p blood types using *Pseudomonas aeruginosa* PA-I lectin. Transfusion. 1996;36:113-6.
2. Tenner AJ, Cooper NR. Identification of types of cells in human peripheral blood that bind C1q. J Immunol. 1981;126:1174-9.
3. Wilson A, Sweeney M, Mark Lynch PL, et al. Hemolysis rates in whole blood samples for blood gas/electrolyte analysis by point-of-care testing. J Appl Lab Med. 2018;3:144-5.
4. Tallman CI, Darracq M, Young M. Analysis of intraosseous blood samples using an EPOC point of care analyzer during resuscitation. Am J Emerg Med. 2017;35:499-501.
5. Neri AJ, Roy J, Jarrett J, et al. Analysis of a novel field dilution method for testing samples that exceed the analytic range of point-of-care blood lead analyzers. Int J Environ Health Res. 2014;24:418-28.
6. Moroff G, Eich J, Dabay M. Validation of use of the Nageotte hemocytometer to count low levels of white cells in white cell-reduced platelet components. Transfusion. 1994;34:35-8.
7. Mangla A, Ehsan M, Agarwal N, et al. Sickle cell anemia. StatPearls, Treasure Island, Florida, USA. 2022.
8. Mangla A, Ehsan M, Agarwal N, et al. Sickle cell anemia (nursing). StatPearls, Treasure Island, Florida, USA. 2022.
9. Arias de la Vega F, Torres López A, Piedra Roset P, et al. Paraneoplastic hemolytic anemia associated with prostate cancer. a case report. An Sist Sanit Navar. 2022;45:e1023.
10. Han X, Ji P. Carbon dots for the treatment of cancer-related anemia. Blood Sci. 2022;4:174-5.
11. Rosenblum WI. Effects of reduced hematocrit on erythrocyte velocity and fluorescein transit time in the cerebral microcirculation of the mouse. Circ Res. 1971;29:96-103.
12. Blumenfeld OO, Huang CH. Molecular genetics of the glycophorin gene family, the antigens for MNSs blood groups: multiple gene rearrangements and modulation of splice site usage result in extensive diversification. Hum Mutat. 1995;6:199-209.
13. Blumenfeld OO, Huang CH. Molecular genetics of glycophorin MNS variants. Transfus Clin Biol. 1997;4:357-65.
14. Fukuda M. Molecular genetics of the glycophorin A gene cluster. Semin Hematol. 1993;30:138-51.
15. Wise GE, Oakford LX, Dzandu JK. Ultrastructure of a transmembrane glycoprotein, glycophorin A. Tissue Cell. 1988;20:219-27.
16. Graham MD. The coulter principle: a history. Cytometry A. 2022;101:8-11.
17. Graham MD. The coulter principle: imaginary origins. Cytometry A. 2013;83:1057-61.
18. Rhyner MN. The Coulter principle for analysis of subvisible particles in protein formulations. AAPS J. 2011;13:54-8.
19. Dijkstra-Tiekstra MJ, Schrijver JG, van der Meer PF, et al. Crossover study of three methods for low-level white blood cell counting on two types of flow cytometer. Cytometry B Clin Cytom. 2003;54:39-45.
20. Tvedten H. What is your diagnosis? Discrepancy in platelet counts determined using a Sysmex XT-2000 iV hematology analyzer. Erroneous PLT-O due to RBC ghosts. Vet Clin Pathol. 2010;39:395-6.
21. Hwang DH, Dorfman DM, Hwang DG, et al. Automated nucleated RBC measurement using the Sysmex XE-5000 Hematology Analyzer: frequency and clinical significance of the nucleated RBCs. Am J Clin Pathol. 2016;145:379-84.

22. Gutmann J, Hofmann G, Ruhenstroth-Bauer G. Exact methods for measuring the volume distribution of erythrocytes on the basis of the Coulter principle. Bibl Haematol. 1966;24:42-53.

23. Luider J, Cyfra M, Johnson P, et al. Impact of the new Beckman Coulter Cytomics FC 500 5-color flow cytometer on a regional flow cytometry clinical laboratory service. Lab Hematol. 2004;10:102-8.

24. O'Neil E, Burton S, Horney B, et al. Comparison of white and red blood cell estimates in urine sediment with hemocytometer and automated counts in dogs and cats. Vet Clin Pathol. 2013;42:78-84.

25. Despotis GJ, Alsoufiev A, Hogue CW Jr, et al. Evaluation of complete blood count results from a new, on-site hemocytometer compared with a laboratory-based hemocytometer. Crit Care Med. 1996;24:1163-7.

26. Frolova AD, Vasil'kovskiĭ VG, Kuznetsova OA, et al. Evaluation of the morphofunctional status of peripheral blood cells using the GTsMK-3 hemocytometer. Lab Delo. 1991;5:9-10.

27. Whittington RJ, Comer DA. Discrepancy between hemocytometer and electronic counts of blood cells. J Wildl Dis. 1984;20:258-60.

28. Hino S. Theory and practice of counting blood cells with hemocytometer. Rinsho Ketsueki. 1978;19:1171-8.

29. Asha SE, Chan AC, Walter E, et al. Impact from point-of-care devices on emergency department patient processing times compared with central laboratory testing of blood samples: a randomised controlled trial and cost-effectiveness analysis. Emerg Med J. 2014;31:714-9.

30. Sang S, Feng Q, Jian A, et al. Portable microsystem integrates multifunctional dielectrophoresis manipulations and a surface stress biosensor to detect red blood cells for hemolytic anemia. Sci Rep. 2016;6:33626.

31. Klein MN, Larkin EJ, Marshall JN, et al. Autoantibodies to red blood cell surface Glycophorin A impact the activation poise of circulating leukocytes. Transfusion. 2022;62:217-26.

32. Young MT, Tanner MJ. Distinct regions of human glycophorin A enhance human red cell anion exchanger (band 3; AE1) transport function and surface trafficking. J Biol Chem. 2003;278:32954-61.

33. Branch DW, Huber DL, Brozik SM, et al. Shear horizontal surface acoustic wave microsensor for Class A viral and bacterial detection (No. SAND2008-6128). Sandia National Laboratories (SNL), Albuquerque, NM, and Livermore, CA, United States. 2008.

34. Guo XS, Chen YQ, Yang XL, et al. Novel shear-horizontal surface acoustic wave based immunosensors using SiO_2 waveguiding layers and flow injection analysis. 2005 IEEE Engineering in Medicine and Biology 27th Annual Conference, Shanghai, China. 2005.

35. Haofeng L, Rui J, Weilong L, et al. Surface acoustic wave sensors of delay lines based on MEMS. J Nanosci Nanotechnol. 2010;10:7258-61.

36. Hashimoto KY. Surface acoustic wave devices in telecommunications: modelling and simulation. Springer Berlin, Heidelberg. 2000.

37. Josse F, Bender F, Cernose RW. Guided shear horizontal surface acoustic wave sensors for chemical and biochemical detection in liquids. Anal Chem. 2001;73:5937-44.

38. Lange K, Gruhl FJ, Rapp M. Surface Acoustic Wave (SAW) biosensors: coupling of sensing layers and measurement. Methods Mol Biol. 2013;949:491-505.

39. Lange K, Rapp BE, Rapp M. Surface acoustic wave biosensors: a review. Anal Bioanal Chem. 2008;391:1509-19.

40. Hu G, Xu J, Auner GW, et al. Viscosity response of shear horizontal surface acoustic wave on AlN/sapphire structure. Electronics Letters. 2013;43:1006-7.

41. Bisoffi M, Hjelle B, Brown DC, et al. Detection of viral bioagents using a shear horizontal surface acoustic wave biosensor. Biosens Bioelectron. 2008;23:1397-403.

42. Yatsuda H. Design techniques for SAW filters using slanted finger interdigital transducers. IEEE Trans Ultrason Ferroelectr Freq Control. 1997;44:453-9.

43. Yatsuda H. Design technique for nonlinear phase SAW filters using slanted finger interdigital transducers. IEEE Trans Ultrason Ferroelectr Freq Control. 1998;45:41-7.

44. Yatsuda H, Yamanouchi K. Automatic computer-aided design of SAW filters using slanted finger interdigital transducers. IEEE Trans Ultrason Ferroelectr Freq Control. 2000;47:140-7.

45. Afzal M, Nawaz R, Ayub M, et al. Acoustic scattering in flexible waveguide involving step discontinuity. PLoS One. 2014;9:e103807.

46. Agostini M, Cecchini M. Ultra-high-frequency (UHF) surface-acoustic-wave (SAW) microfluidics and biosensors. Nanotechnology. 2021;32:312001.

47. Alvarez M, Friend J, Yeo LY. Rapid generation of protein aerosols and nanoparticles via surface acoustic wave atomization. Nanotechnology. 2008;19:455103.

48. Arimoto A, Muraoka K, Shimano T, et al. Waveguide optical deflector for an optical disk tracking actuator using a surface acoustic wave device. Appl Opt. 1990;29:247-50.

49. Viespe C, Miu D. Characteristics of surface acoustic wave sensors with nanoparticles embedded in polymer sensitive layers for VOC detection. Sensors. 2018;18:2401.